NASA LANGLEY AIRBORNE HIGH SPECTRAL RESOLUTION LIDAR INSTRUMENT DESCRIPTION

David .B. Harper[(1)], Anthony Cook[(1)], Chris Hostetler[(1)], John W. Hair[(1)], Terry L. Mack[(2)]

[(1)] NASA Langley Research Center, MS468 Hampton, Virginia, 23681-2199, USA, David.B.Harper@nasa.gov
[(2)] Lockheed Martin, MS473 Hampton, Virginia, 23681-2199, USA, Terry.L.Mack@nasa.gov

ABSTRACT

NASA Langley Research Center (LaRC) recently developed the LaRC Airborne High Spectral Resolution Lidar (HSRL) to make measurements of aerosol and cloud distribution and optical properties. The Airborne HSRL has undergone as series of test flights and was successfully deployed on the Megacity Initiative: Local and Global Research Observations (MILAGRO) field mission in March 2006 (see Hair et al. in these proceedings). This paper provides an overview of the design of the Airborne HSRL and descriptions of some key subsystems unique to this instrument.

1 INSTRUMENT OVERVIEW

A functional block diagram of the HSRL instrument is shown in Fig.1. The Airborne HSRL operates as a high spectral resolution lidar at 532 nm using the iodine vapor filter technique [1-2] and a backscatter lidar at 1064 nm. Depolarization is measured at both wavelengths.

The laser transmitter consists of four basic components: an Nd:YAG CW seed laser, an electro-optic feedback loop that locks the seed laser to an iodine absorption line, and an injection-seeded pulsed Nd:YAG laser slaved to the seed [3] and an output conditioning module that provides control over beam steering, output power, and polarization orientation. The seed laser and pulsed slave laser were developed by Innolight GmbH and Fibertek, Inc., respectively. The electroptic control loop and the output conditioning modules were designed and implemented by LaRC.

The receiver employs a 16-inch Newtonian telescope to which an aft-optics module is kinematically mounted. The aft optics module separates wavelengths, filters the return to reject out-of-band background light, and separates polarization components. The 532 nm parallel-polarized backscatter is further split in the aft optics module: approximately 4% of the 532 parallel return is sent to the boresight subsystem which automatically maintains alignment between the transmit and receive optical axes; approximately 10% of the parallel backscatter is transferred directly to the detector subsystem; and the remaining 86% of the parallel 532 nm backscatter is directed to the iodine vapor filter module which provides rejection of the Mie component of the backscatter. The 10% channel measures total (molecular plus aerosol) parallel backscatter and the 86% channel is sensitive to only the

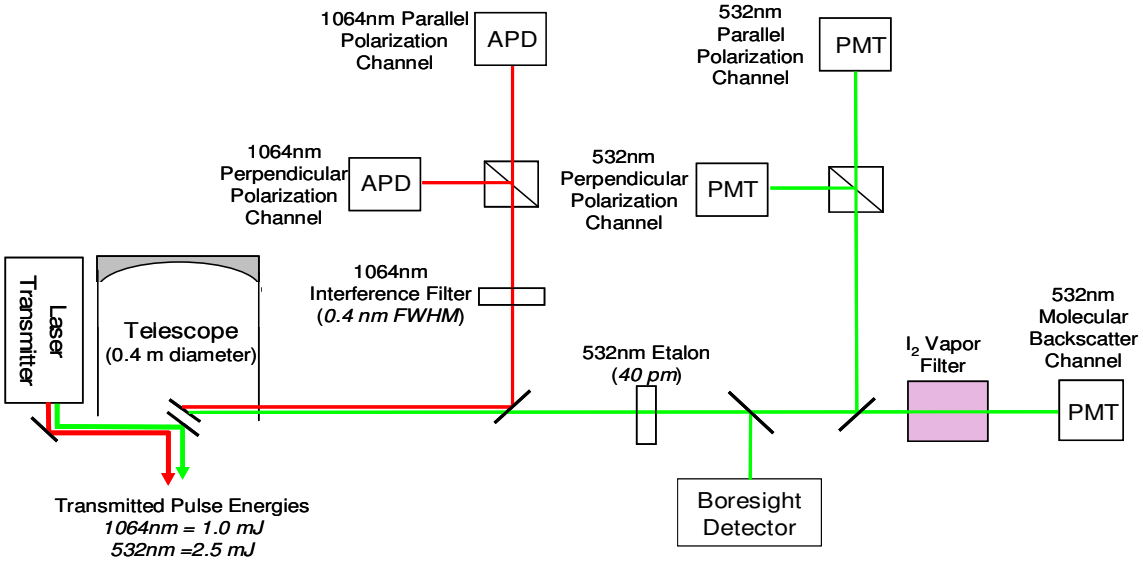

Fig. 1. HSRL Functional Diagram

molecular backscatter. The resulting optical channels are fiber-optically coupled to the various detector subsystems.

2 LASER FREQUENCY LOCKING

The HSRL technique as employed in this system relies on stable locking of the transmitted laser frequency to the center of an iodine absorption line. Frequency locking of the pulsed laser output is accomplished by controlling the frequency of the CW seed laser. A piezo element on the seed laser crystal provides fast frequency tuning and a thermo-electric cooler (TEC) provides slow frequency tuning. The signals that drive the piezo element and the TEC which control the seed laser wavelength are generated in an electro-optic feedback loop involving the frequency doubled seed output at 532 nm.

A block diagram of the laser frequency locking subsystem is shown in Fig. 2. The 532 nm output from the seed laser is phase modulated to produce sidebands that are at ± 240MHz about 532-nm output frequency [4]. The phase modulated output is passed through an iodine vapor cell where the intensity of the center and sideband frequencies are attenuated by varying degrees depending upon the difference between the doubled seed laser frequency and the center of the iodine absorption line. When the doubled seed frequency is centered on the iodine line, the power in the two sidebands is equal; when the seed is not centered on the iodine line, a mismatch in sideband power is produced. The optical signal from the phase modulator (i.e., the doubled laser frequency and the two sidebands) is incident onto a silicon detector. The output of the detector is amplified, passed through a phase shifter, and mixed with the original 240 MHz signal used to drive the phase modulator. The output of the mixer produces an error signal that is proportional to the difference of the doubled seed laser frequency and the center frequency of the iodine absorption line.

The error signal from the frequency mixer is fed into a dual proportional-integral (PI) controller circuit to vary the frequency of the seed laser. The first PI controller sets the output signal to the piezo element providing fast tuning of the seed laser output. However, the dynamic range of the piezo element is limited, and temperature drifts in the seed laser can put the optimal control position beyond the range of the piezo element. Therefore, a second PI loop is used to monitor the piezo control output, adjusting the seed laser crystal temperature as needed to keep the piezo control output within limits.

3 SPECTRAL PURITY

In addition to precise output frequency control, the HSRL technique relies upon high spectral purity of the output: i.e., the power in the main laser mode centered on the iodine absorption line must exceed the power of modes off line center by orders of magnitude. Otherwise, the signal measured in the "molecular channel" downstream of the iodine cell in the receiver (different from the iodine cell in the frequency locking subsystem) would include excessive Mie backscatter, invalidating the assumptions inherent in the retrieval of extinction. (We note that this Mie cross-talk could be characterized and incorporated in the retrieval; however, a system that provides nearly complete

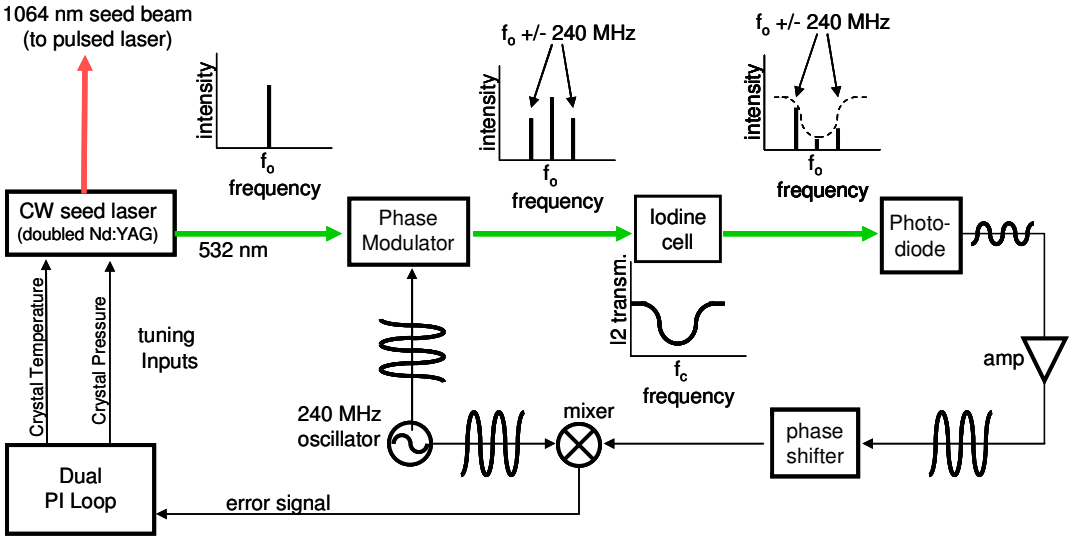

Fig. 2. HSRL Laser Frequency Locking System

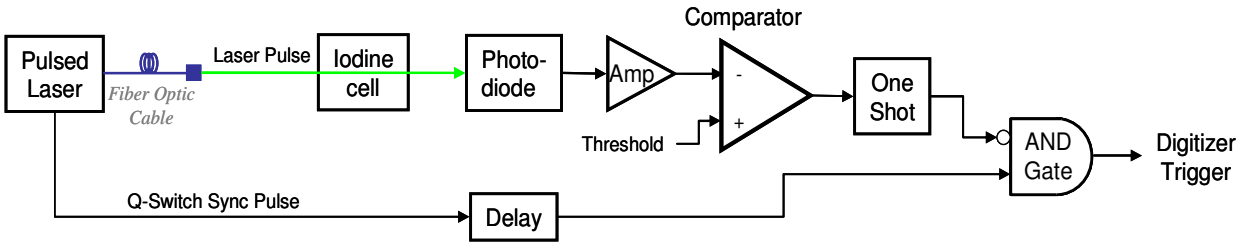

Fig. 3. Spectral Purity Detector System

rejection of the Mie backscatter can be more easily calibrated and provide a measurement with lower systematic error.)

Although the laser frequency locking system is very robust and performs well, a decision was made during the design phase of the instrument to add a subsystem for measuring the spectral purity of the pulsed laser output to insure that the system was performing as designed on a shot-to-shot basis. When the system detects a laser shot that is not spectrally pure, it over-rides the digitizer trigger and prevents the offending profile from being recorded.

The block diagram of the spectral purity detection subsystem is shown if Fig. 3. A fraction of the transmitted pulsed 532 nm laser beam (~0.5%) is picked off and delivered to the spectral purity subsystem via optical fiber. The light exiting the fiber is collimated and passed through an iodine vapor cell (separate from the cells in the laser locking and receiver subsystems) and then focused onto a detector. When the laser is operating on a single longitudinal mode centered on an iodine absorption line (line center transmission value of 10^{-6}) the light in the spectral purity subsystem is effectively extinguished in the iodine cell. When the laser is operating off line center and/or other longitudinal modes are propagating, light passes through the cell, producing a large pulse at the output of the detector. The output pulse from the detector is amplified and sent to a comparator where an experimentally determined discrimination threshold is implemented. Detected pulses with amplitudes above the threshold, hence not spectrally pure, will trip the comparator and gating logic, thereby effectively defeating the digitizer trigger as shown if Fig 3. Under typical conditions, the measured spectral purity of the system (ratio of offline to online transmission through the spectral purity iodine cell) is greater than 5000:1, and the spectral purity system screens zero shots.

4 IODINE FILTER CALIBRATION

To provide a near real-time, internally calibrated measurement of backscatter at 532 nm, the absorption line shape and absolute transmission of the iodine vapor filter in the receiver is measured periodically. Figure 4 shows the receiver iodine filter and calibration subsystem. The filter and calibration system are housed in a light-tight enclosure which includes three separate optical paths and detectors. The PMT is the science channel detector and the iodine cell is positioned upstream of this detector during science data acquisition. During calibration operations, the iodine cell is moved to the position in front of the PIN diode labeled PIN 1, and 532 nm CW light from the seed laser is directed through the cell to PIN 1 and through an open path to PIN 2. The seed laser frequency is tuned to scan through the iodine line chosen for the measurement. PIN 1 measures the relative shape of the line and PIN 2 provides a reference for calculating the transmission through the cell. A confocal interferometer (not shown) is used to provide frequency markers and determine the frequency scan range of the seed laser during the scan.

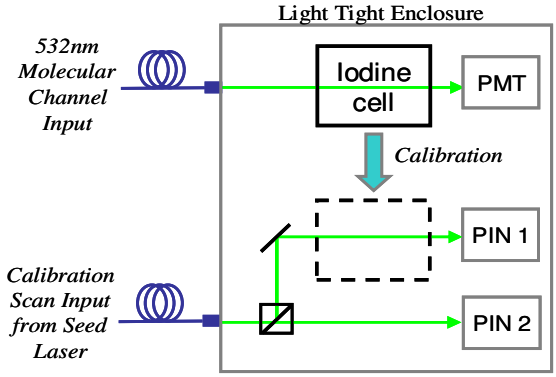

Fig. 4. Iodine Filter Calibration System

The receiver iodine cell was built and implemented as a "starved cell": a fixed amount of iodine was introduced into the cell before sealing and the cell is heated such that all the iodine molecules are in the gas phase (56º in this system). Implemented as such, the line shape and transmission of the cell are determined solely by Doppler broadening and pressure broadening linewidth changes that are a function of the cell temperature and pressure, and not variations in iodine density [5]. Measurements of the iodine filter spectrum have shown

that the transmission is extremely stable: better than 1% over the range of the molecular scattering spectrum (+/- 5 GHz). Table 1 shows the molecular scattering transmission through the filter (~29%) based on the iodine transmission values measured for the specified dates.

Table 1: Molecular scattering (275K, 0.75Pa) transmission through cell based on the measured iodine filter spectrum for the given dates.

Transmission	Date
0.290	9/15/2004
0.283	10/14/2005
0.281	4/24/2006

5 ACTIVE BORESIGHT SYSTEM

The HSRL instrument utilizes a unique quadrant detector to measure the pointing error of the transmitted laser with respect to the receiver field of view. Typical lidar boresight systems image the field stop on a quadrant PMT or APD to determine boresight error signals as shown in Fig. 5.

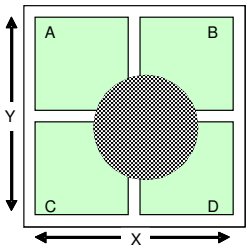

Fig. 5. Typcial Quadrant Detector

$$x_o = \frac{(B+D)-(A+C)}{A+B+C+D} \quad (1)$$

$$y_o = \frac{(A+B)-(C+D)}{A+B+C+D} \quad (2)$$

There are issues which complicate the use of quadrant or multi-element PMT and APD detectors [6], however. The size of commercially available quadrant detectors is very limited, imposing undesirable constraints on the optical design of the system. Also, the dead zone between quadrants is much larger than desired (at least for our optical configuration) and there can often be a large spatial variation in responsivity over the detector active area. It was believed that these issues could lead to large systematic errors in the boresight control signals and reduce the achieved pointing accuracy/stability. To avoid these complications, the Airborne HSRL boresight detection subsystem was implemented using a novel quad fiber bundle rather than a quad detector. Each quadrant is a bundle of hundreds of fibers with a 25 um diameter core. The output end of each quadrant bundle is spatially randomized and split out to a separate SMA fiber connector. The quad fiber bundle can be fabricated to be up to many millimeters in diameter; the diameter of the quad fiber used in the Airborne HSRL is 4.7 mm. The 10 μm dead space between fiber quadrants is much smaller than available in commercial quad detectors and the spatial randomization of the individual fibers within each quad bundle eliminates spatial variability of sensitivity at the field stop image. The light from each quad bundle is allowed to diverge onto a separate single-element large-area PMT, where the signal is amplified, filtered, and digitized. A software loop running on the data acquisition computer calculates the pointing error according to (1) and (2) and feeds that error into a PI control loop to determine the corrective laser beam steering output.

6 REFERENCES

1. Piironen, P. and E. W. Eloranta, "Demonstration of a High-Spectral-Resolution Lidar based on a Iodine Absorption Filter". *Optics Letters*, **19**, 3, 234-236, 1994.
2. Z. Liu, I. Matsui, and N. Sugimoto, "High-spectral-resolution lidar using an iodine absorption filter for atmospheric measurements," Opt. Eng. **38,** 1661–1670, 1999.
3. Floyd E. Hovis, Michael Rhoades, Ralph L. Burnham, Jason D. Force, T. Schum, Bruce M. Gentry, Huailin Chen, Steven X. Li, Johnathan W. Hair, Anthony L. Cook, Chris A. Hostetler, "Single-frequency lasers for remote sensing", Proc. SPIE Vol. 5332, p. 263-270, Solid State Lasers XIII: Technology and Devices; Richard Scheps, Hanna J. Hoffman; Eds., July 2004.
4. A. Arie and R. L. Byer, "Frequency stabilization of the 1064 nm Nd:YAG lasers to Doppler-broadened lines of iodine", *Applied Optics* , **32**, 7382-7386, 1993.
5. Crafton, Jim, Campbell D Carter, and Gregory S Elliott, "Three-component phase-averaged velocity measurements of an optically perturbed supersonic jet using multi-component planar Doppler velocimetry", *Meas. Sci. Technol.* **12** 409–419, 2001.
6. Sharmin, Paul, 'Position sensing with photodiodes' *Laser Focus World* February, 2002.